

Optical performance at the thermodynamic limit with tailored imaging designs

Jeffrey M. Gordon and Daniel Feuermann

Ultracompact concentrators and illuminators that approach the thermodynamic limit to optical performance can be realized with purely imaging strategies. We explore two-stage reflector systems where each optical surface is tailored to eliminate one order of aberration—the so-called aplanatic designs. The contours are monotonic functions that can be expressed analytically, which are important for the facilitation of optimization studies and practical fabrication. The radiative performance of the devices presented is competitive with, and even superior to, that of high-flux nonimaging systems. Sample results of practical value in solar concentration and light collimation are presented for systems that cover a wide range of numerical aperture. © 2005 Optical Society of America

OCIS codes: 080.2470, 220.1770, 350.6050.

1. Introduction

Concentrators and illuminators capable of approaching the thermodynamic limit to radiative transfer have commonly been regarded within the realm of nonimaging optics.¹ The alternative of a purely imaging strategy in which each of two mirrored contours is tailored to eliminate one order of aberration was presented in Ref. 2, which included a sample solar concentrator design capable of realizing flux levels above those of even the best nonimaging designs.

The elimination of an order of geometric aberration provides a degree of freedom for tailoring an optical surface. For example, a paraboloidal reflector or a plano-convex lens removes zeroth-order (spherical) aberration. If two surfaces can be tailored, then both zeroth- and first-order (comatic) aberration can be overcome (referred to as aplanatic). Although high-definition, high- f -number imaging systems have in-

corporated aplanatic devices, to our knowledge the value of such double-tailored systems for radiation concentration or collimation has remained unexplored. (The viewpoint and nomenclature of concentrators are adopted in the analysis that follows, although the application to illumination is straightforward as addressed in Section 5.)

Our foray into pure imaging reflector strategies for high-flux applications is motivated by the practical value of simultaneously satisfying (1) ultracompactness, (2) maximum concentration at high collection efficiency, (3) allowing a sizable gap between the absorber and the mirrors, (4) an upward-facing absorber, and (5) obviating chromatic aberration. Nonimaging optical designs are typically not compact and do not accommodate a large gap at the receiver, unless a significant loss in either efficiency or concentration is incurred.¹ Common parabolic and Cassegrain designs provide some, but not all, of these goals. For example, high- f -number systems exhibit small aberrations, but require large aspect ratios and generate low flux. Although compactness and high flux can be achieved with Cassegrains, they incur excessive shading.^{3,4}

Recent progress in maximum-performance solar concentrators,^{5–9} and in collimation for light-emitting diodes and fiber-optic applications, motivate our exploration of the notions portrayed in Ref. 2. The calculational methods depicted in Ref. 2 are cumbersome, but analytic solutions for the mirror contours are now available and markedly facilitate the analysis of a broad range of high-performance optical designs. Our studies are restricted to a far-

The authors are with the Department of Solar Energy and Environmental Physics, Jacob Blaustein Institute for Desert Research, Ben-Gurion University of the Negev, Sede Boqer Campus 84990, Israel. J. M. Gordon (jeff@bgu.ac.il) is also with the Pearlstone Center for Aeronautical Engineering Studies, Department of Mechanical Engineering, Ben-Gurion University of the Negev, Beersheva 84105, Israel, and the School of Natural Sciences and School of Engineering, University of California, Merced, California 95344.

Received 10 November 2004; revised manuscript received 19 November 2004; accepted 19 November 2004.

0003-6935/05/122327-05\$15.00/0

© 2005 Optical Society of America

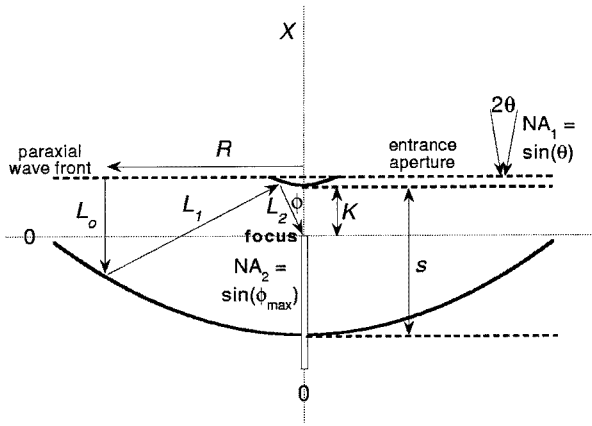


Fig. 1. Illustration of concentrator design. Mirror contours are tailored such that all paraxial rays are focused and the Abbe sine condition is satisfied. Irradiation from the actual extended far-field source has $NA_1 = \sin(\theta)$, to be concentrated onto an extended, upward-facing disk, depicted here as the entrance to an equidiameter light guide. In illumination mode, light emitted over NA_2 from a point focus would emerge perfectly collimated; but the actual illuminator has an extended source and emits over NA_1 .

field source. The near-field problem will be broached in a future study, prompted in part by the needs of modern projection systems, as well as light-based fiber-optic surgical applications with ultrabright incoherent light.¹⁰

2. Design Formalism

Figure 1 portrays the tailoring of axisymmetric imaging mirrors for concentrating uniform radiation with numerical aperture NA_1 onto a flat single-sided absorber at an exit NA_2 . The constrained thermodynamic limit to flux concentration is^{1,11}

$$C_{\max} = (NA_2/NA_1)^2. \quad (1)$$

Therefore the absorber diameter should not be less than

$$d_{\min} = D(NA_1/NA_2), \quad (2)$$

where D denotes the entrance diameter. Larger absorber diameters can raise the collection efficiency, but at the expense of diminished average flux concentration. This fundamental trade-off between concentration and collection efficiency is quantified in Section 4 for an assortment of tailored imaging designs.

Satisfying Fermat's constant-string-length prescription and Abbe's sine condition constitutes the correction for zeroth- and first-order aberrations, respectively^{1,2}:

$$L_0 + L_1 + L_2 = \text{constant}, \quad (3)$$

$$R = (\text{constant}') \sin(\phi), \quad (4)$$

where L denotes the string length, R is the radial

coordinate at the entrance aperture, and ϕ is the angle at which a ray reaches the focus [$NA_2 = \sin(\phi_{\max})$, established by the extreme ray from the primary mirror's rim]. The focus is selected as the origin of the coordinate system (and can lie near or even behind the apex of the primary for sufficiently low NA_2). One then incorporates Snell's law of reflection (a differential equation) and specifies two geometric parameters that we choose as the distances between the apex of the primary and secondary (s) and the focus and the apex of the secondary (K).

A method to solve these coupled equations analytically was recently presented.^{12,13} The parametric solution for the axial (X) and radial (R) coordinates for the primary (subscript p) and secondary (subscript s) shapes is

$$\begin{aligned} R_p &= \frac{2T}{1+T^2}, \\ X_p &= s - \frac{1}{1+T^2} + \frac{[s - (1-s)T^2][1 - Kg(T)]}{s(1+T^2)^2}, \\ R_s &= \frac{2sKTg(T)}{s - (1-s)T^2 + KT^2g(T)}, \\ X_s &= -\frac{sK(1-T^2)g(T)}{s - (1-s)T^2 + KT^2g(T)}, \end{aligned} \quad (5)$$

where

$$T = \tan(\phi/2), \quad g(T) = \left| 1 - \frac{(1-s)T^2}{s} \right|^{\frac{-s}{1-s}}.$$

The radius of the primary is NA_2 . Equations (5) are the solution on one side of the optic axis; the other half is its mirror image. Mathematically valid but physically inadmissible designs exist (numerous examples appear in Refs. 12 and 13), but are not examined here. We impose the pragmatic constraint that shading losses not exceed 0.03. In addition, only designs with negligible blocking losses (i.e., rays reflected from the primary that strike the light guide) are presented.

3. Complementary Solutions

The analysis above, as well as that of Ref. 2, comprise a diverging optical system, i.e., the caustic of rays from the primary resides behind the secondary. There is also a second class of complementary converging solutions, where the caustic lies between the primary and the secondary (and the secondary is always concave). The solution of Eqs. (5) is the same, but with negative values for the geometric input parameters (Fig. 2).

Some cases can result in substantial losses:

- (a) the caustic of rays from the primary can oc-

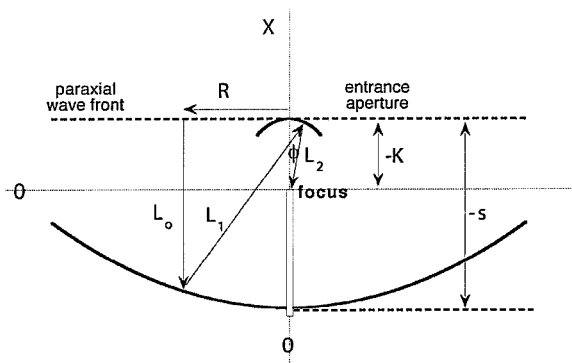


Fig. 2. Design for converging complementary devices (here with $NA_2 = 0.5$), in analogy to Fig. 1.

copy the vicinity of the exterior of the secondary, so that rays from the primary strike the outside of the secondary—exceedingly so for compact units and high NA_2 ;

(b) the secondary can fall below the entrance aperture of the primary, in which case a significant fraction of rays from the primary is lost on the exterior of the secondary; and

(c) as $NA_2 \rightarrow 1$, the overlap between the bottom of the absorber and the caustic can produce considerable blocking.

Because our analyses revealed that, relative to diverging designs, converging solutions enjoy neither any practical or flux performance advantage nor greater tolerance to optical errors, the examples given in Section 4 are restricted to diverging solutions.

4. Optical Performance

Optical performance was ascertained with simulations¹⁴ in which 250,000 rays distributed uniformly both spatially and in solid angle were traced, with a top-hat angular input distribution. Results are summarized as flux maps for a particular concentrator with varying NA_1 values (Fig. 3). (To avoid ambiguity in the length scale for the different cases in Fig. 3, the radius of each primary dish is defined as unity.)

Characteristic plots of efficiency against concentration⁴ (Fig. 4) follow from flux map integration. Efficiency remains less than unity even in the low-concentration regime due to ray rejection and shading. Absorption in the (specular) reflectors is not included but is readily estimated as $1-\rho^2$ (ρ is the reflectivity) since each ray experiences exactly two reflections. Fresnel reflections from the absorber are also not accounted for since they are material specific and easily quantified.

NA_1 represents the convolution of the actual source size with optical errors. With solar concentrators in mind, ray-trace simulations were performed for $NA_1 \geq 0.005$ because the solar disk subtends an angular radius of 0.0047 rad and optical errors commensurate with $NA_1 = 0.005$ are experimentally

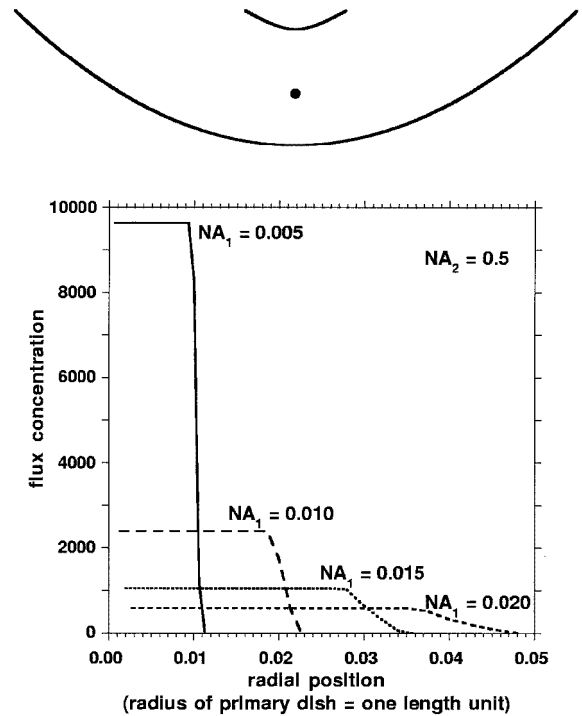


Fig. 3. Tailored imaging concentrator designed for $NA_2 = 0.50$. The absorber is sited in the focal plane (the solid dot indicates the focus). Flux maps are plotted for a range of NA_1 values.

attainable.¹⁵ The largest NA_1 value of 0.020 subsumes liberal errors in mirror contour and alignment.

No special significance should be attached to the NA_2 values chosen for Fig. 4 [except in Fig. 4(c) toward demonstrating that practical devices are possible at the ultimate flux limit of $NA_2 = 1.00$]. Figures 4(a) and 4(b) were motivated by recent progress in high-flux photovoltaic devices,^{6,9} where we aimed to satisfy the five objectives listed in Section 1. These are cases in which practical systems need to accommodate optical tolerances of affordable manufacturing procedures, as well as net flux concentration values in the range of 300–2000 suns. Both ultracompactness (aspect ratios of close to 1/4) and coplanarity of the rims of the primary and secondary essential to certain low-cost high-volume production techniques¹⁶ are also achievable. [The $NA_2 = 0.50$ design of Figs. 3 and 4(b) satisfies coplanarity and compactness, but requires siting the focus above the apex of the primary to avoid shading losses exceeding 0.03.]

The optical performance of imaging concentrators will worsen as NA_1 grows and higher-order aberrations are magnified. The sensitivity to NA_2 and to compactness is subtler. As NA_2 is raised, it becomes increasingly difficult to realize compact configurations without introducing excessive shading or ray rejection. Deeper concentrators tend to be more tolerant to larger NA_1 . Similarly, a larger secondary reduces the sensitivity to NA_1 , but at the expense of greater shading.

Efficiency-concentration relations for tailored imaging designs are superior to those of corresponding

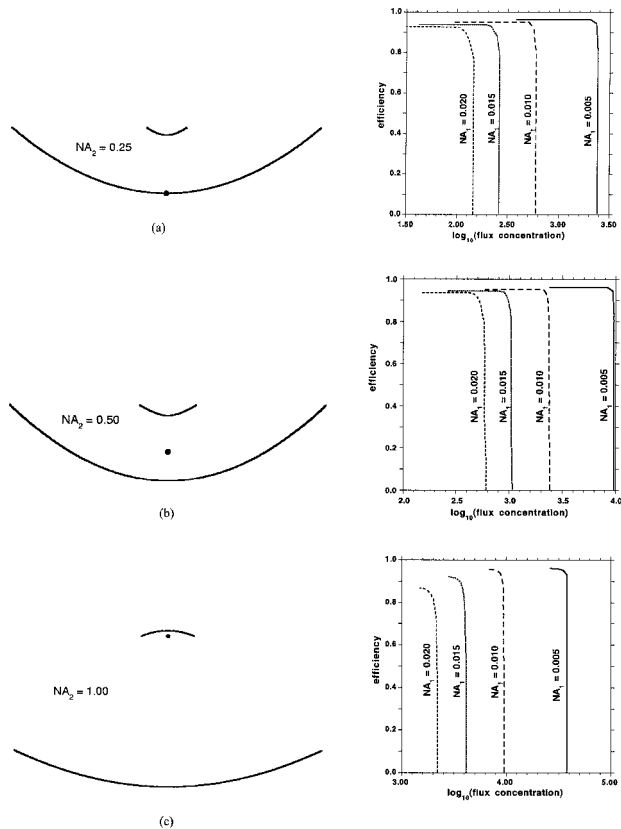


Fig. 4. Sample tailored imaging concentrators and their efficiency concentration curves.

conventional imaging devices. This would appear to derive from the dependence of aberrations on the f -number (f). First-order aberration is proportional to f^2 , whereas second-order aberration is proportional to $1/f$ (the reason that compact conventional imaging systems incur severe coma).¹² It also explains why the most compact tailored imaging concentrators with low shading are least tolerant to increasing NA_1 .

5. Collimators

In illumination mode, a quasi-Lambertian source emitting over NA_2 sits at the focus. Collimation is required over a nominal NA_1 (at high efficiency). NA_1 for the actual illuminator comprises the convolution of the extended source with optical errors. The source could, for example, be an optical fiber or a light-emitting diode and would be sized based on the prescribed NA_1 , with the minimum source size following from the restricted thermodynamic limit [Eq. (2)].

The design of Fig. 4(b) (in illumination mode) offers an illustrative example. The flux maps of Fig. 5 summarize the ray-trace results. The angular dependence of irradiance is the same at near and far field here because the distinguishing factor of $\cos^4(\theta)$ for far-field illuminance is essentially unity ($NA_1 \leq 0.020$). The resemblance between flux maps in concentrator and collimator mode follows from the relation between the concentrator acceptance angle function and the collimator far-field illuminance.¹⁷

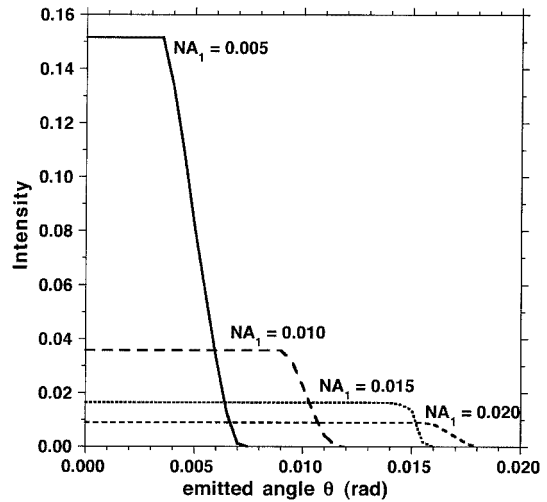


Fig. 5. Flux maps when the design of Fig. 4(b) is deployed as a collimator. Intensity I is scaled such that $I I(\theta) d[\sin^2(\theta)]$ equals the efficiency.

Radiative losses stem from

- (1) trapped rays that either exit through the apex region of the primary or are reflected to the base of the source (analogous to shading losses in concentrators);
- (2) off-axis rays from the periphery of the source that miss the secondary (zero-reflection emissions); and
- (3) off-axis rays reflected to large emission angles.

The latter two categories can be decreased by modest overdesign, e.g., by slightly increasing the design value of NA_2 relative to the NA_2 of the actual light source. The ray-trace results portrayed in Fig. 6 relate to a collimator with a moderate overdesign: The actual source possesses $NA_2 = 0.46$ but the design is for $NA_2 = 0.50$, with a target collimation $NA_1 = 0.010$.

6. Discussion

We have explored the ability of purely imaging two-stage concentrators and illuminators to provide radiative transfer at the thermodynamic limit. Their mirror contours are tailored to eliminate zeroth- and first-order aberrations in devices devoid of chromatic aberration. When the NA of far-field sources or targets does not exceed around 0.02, these aplanatic systems outperform even the best nonimaging counterparts. Their practical virtues include ultracompactness (aspect ratios close to 1/4) and the ability to accommodate a large gap between the focus and the mirrors. The reflector shapes are monotonic functions that can be expressed analytically, which is important in both tenable optimization studies and affordable manufacturing procedures. Case studies that cover a wide range of NA reveal both the robustness and the limitations of such devices.

Although the devices analyzed here are axisymmetric, optical systems may require different shapes

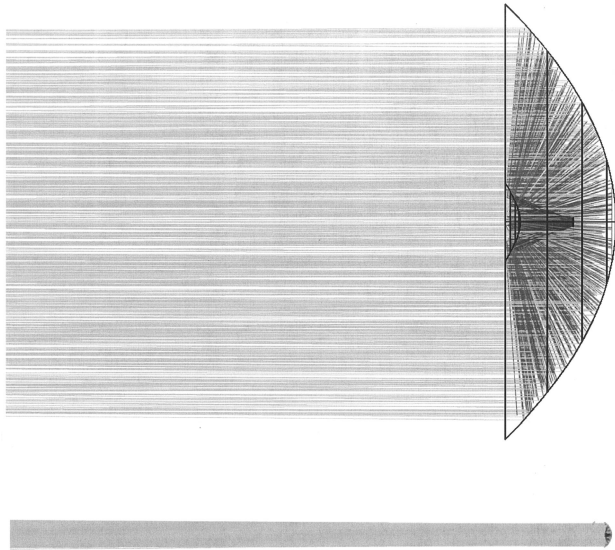


Fig. 6. Illustration of collimation performance. The actual source has $NA_2 = 0.46$, but the illuminator is slightly oversized for $NA_2 = 0.50$. The intended collimation is $NA_1 = 0.010$. The upper and lower drawings pertain to near- and far-field targets, respectively.

for the absorber or entrance aperture. Flux uniformity may also be crucial. Solutions are available for such modifications in geometry and range from light guides that accommodate the geometric conversion, albeit at a dilution in concentration,^{18,19} to micro-groove structures that achieve the shape conversion at minimal reduction in flux.²⁰ Such constructions can modify the tailored imaging designs described here and, in the spirit of economy of presentation, are delegated to future case-specific studies.

We acknowledge the design challenges in high-flux photovoltaic concentrators provided by Steve Horne and Gary Conley of H₂Go Inc. (Saratoga, California), as well as their support of our research and their commercial development of maximum-performance tailored imaging photovoltaic concentrators. All line drawings in this paper are reproduced from Ref. 21 with the publisher's (Society of Photo-Optical Instrumentation Engineers') permission.

References

1. W. T. Welford and R. Winston, *High Collection Nonimaging Optics* (Academic, San Diego, Calif., 1989).
2. H. Ries and J. M. Gordon, "Double tailored imaging concentrators," in *Nonimaging Optics: Maximum Efficiency Light Transfer V*, R. Winston, eds., Proc. SPIE **3781**, 129–134 (1999).
3. C. E. Mauk, H. W. Prengle, and C. H. S. Eddy, "Optical and thermal analysis of a Cassegrainian solar concentrator," *Sol. Energy* **23**, 157–167 (1979).
4. D. Feuermann, J. M. Gordon, and H. Ries, "High-flux solar

- concentration with imaging designs," *Sol. Energy* **65**, 83–89 (1999).
5. D. Feuermann and J. M. Gordon, "Solar fiber-optic mini dishes: a new approach to the efficient collection of sunlight," *Sol. Energy* **65**, 159–170 (1999).
6. D. Feuermann and J. M. Gordon, "High-concentration photovoltaic designs based on miniature parabolic dishes," *Sol. Energy* **70**, 423–430 (2001).
7. J. M. Gordon, D. Feuermann, and M. Huleihil, "Laser surgical effects with concentrated solar radiation," *Appl. Phys. Lett.* **81**, 2653–2655 (2002).
8. J. M. Gordon, D. Feuermann, M. Huleihil, and E. A. Katz, "New optical systems for the solar generation of nanomaterials," in *Nonimaging Optics: Maximum Efficiency Light Transfer VII*, R. Winston, ed., Proc. SPIE **5185**, 99–108 (2003).
9. J. M. Gordon, E. A. Katz, D. Feuermann, and M. Huleihil, "Toward high-flux photovoltaic concentration," *Appl. Phys. Lett.* **84**, 3642–3644 (2004).
10. D. Feuermann, J. M. Gordon, H. Ries, K. C. Ng, H. T. Chua, and M. Altura, "System and apparatus for photothermal and photochemical medical treatments with incoherent light," U.S. Patent and Patent Cooperation Treaty, International Publication W02004/1105576A1 (2004).
11. A. Rabl, "Comparison of solar concentrators," *Sol. Energy* **18**, 93–111 (1976).
12. D. Lynden-Bell, "Exact optics: a unification of optical telescope design," *Mon. Not. R. Astron. Soc.* **334**, 787–796 (2002).
13. R. V. Willstrop and D. Lynden-Bell, "Exact optics. II. Exploration of designs on- and off-axis," *Mon. Not. R. Astron. Soc.* **342**, 33–49 (2003).
14. OptiCAD, Version 9.1 (OptiCAD Corp., Santa Fe, N.M., 2003).
15. D. Feuermann, J. M. Gordon, and M. Huleihil, "Solar fiber-optic mini-dish concentrators: first experimental results and field experience," *Sol. Energy* **72**, 459–472 (2002), Erratum, **73**, 73 (2002).
16. S. Horne and G. Conley, "Concentrating photovoltaic system: an engineering overview," H₂GO Corp. Internal Technical Report (H₂GO Corp., Saratoga, Calif., 2004).
17. J. M. Gordon, P. Kashin, and A. Rabl, "Nonimaging reflectors for efficient uniform illumination," *Appl. Opt.* **31**, 6027–6035 (1992).
18. K. Araki, M. Kondo, H. Uozumi, Y. Kemmoku, T. Egami, M. Hiramatsu, Y. Miyazaki, N. J. Ekins-Daukes, and M. Yamaguchi, "A 28% efficient, 400-sun concentrator module and its packaging technologies," presented at the International Solar Concentrator Conference for the Generation of Electricity or Hydrogen, NREL/CD-520-35349, Alice Springs, Australia, 10–14 November, 2003.
19. H. Ries, J. M. Gordon, and M. Lasken, "High-flux photovoltaic concentrators with kaleidoscope-based optical designs," *Sol. Energy* **60**, 11–16 (1997).
20. R. Leutz, F. Ling, and H. Ries, "Secondary optics for solar concentrators," presented at the International Solar Concentrator Conference for the Generation of Electricity or Hydrogen, NREL/CD-520-35349, Alice Springs, Australia, 10–14 November 2003.
21. J. M. Gordon and D. Feuermann, "Tailored imaging optics for concentration and illumination at the thermodynamic limit," in *Nonimaging Optics and Efficient Illumination Systems*, R. Winston and J. R. Koshel, eds., Proc. SPIE **5529**, 130–139 (2004).